www.sciencemag.org/content/353/6296/399/suppl/DC1

Supplementary Materials for

Cdk5 disruption attenuates tumor PD-L1 expression and promotes antitumor immunity

R. Dixon Dorand, Joseph Nthale, Jay T. Myers, Deborah S. Barkauskas, Stefanie Avril, Steven M. Chirieleison, Tej Pareek, Derek W. Abbott, Duncan S. Stearns, John J. Letterio, Alex Y. Huang,* Agne Petrosiute*

*Corresponding author. Email: ayh3@case.edu (A.Y.H.); axp125@case.edu (A.P.)

Published 15 July 2016, *Science* **353**, 399 (2016)
DOI: 10.1126/science.aae0477

This PDF file includes

Other Supplementary Material for this manuscript includes the following:
(available at www.sciencemag.org/content/353/6296/399/suppl/DC1)

Excel tables
Table S1. shCdk5-All phosphoproteomics data
Table S2. shCdk5-Significant phosphoproteomics data
Table S3. crCdk5-All phosphoproteomics data
Table S4. crCdk5-Significant phosphoproteomics data

Materials and Methods

Mice

Male B6 nude mice (B6.Cg/NTac-*Foxn1*^{nu} NE10) were obtained from Taconic, and male C57BL/6J, MHC-II KO and β2M KO mice were obtained from The Jackson Laboratory (Bar Harbor, ME). NSG mice were obtained from the Athymic Animal and Xenograft Core Facility of the Case Comprehensive Cancer Center. Animals were housed, bred and handled in the Animal Resource Center facilities at Case Western Reserve University according to approved protocols. All animal experiments were performed in 6- to 12-week old animals with strict adherence to the active experimental protocols approved by the Institutional Animal Care and Use Committee.

Cell Culture

The following cell lines were used in this study: mouse MB cell lines MM1, MM2, MM3 and MM5, derived from *Patched*$^{+/-}$/*p53*$^{-/-}$ mice were obtained from G. Plautz (the Cleveland Clinic). Human MB cell lines DAOY, UW228, D283 and D425 were available in our tumor repository. Human RMS cell line SJCRH30 was purchased from ATCC (CRL-2061). Mouse RMS76.9 was generously provided by C. Mackall (NCI/NIH). All cells were grown in RPMI supplemented with 10% FBS.

Cdk5 & PD-L1 Gene Silencing in Tumor cells

Endogenous Cdk5 gene expression in MM1 was silenced using commercially available Cdk5-targeting antisense shRNAs (Thermo Scientific Open Biosystems cat# RMM4532-EG12568) or by designing CRISPR/Cas9 guide RNAs to edit the Cdk5 locus. Antisense GAPDH, or non-silencing shRNA or crNeg constructs were used as controls. Viral particles were generated in HEK293T cells and used to transduce MM1. Gene targeting was validated by western blotting for both shRNA and CRISPR silencing or qPCR in the case of shRNA silencing. For shRNA Cdk5 silencing, a construct with the antisense sequence, TTGAGTAGACAGATCTCCC, afforded 70% gene knockdown relative to wild type and shNS control and was used to generate MM1 shCdk5 cells. CrisprCdk5_92-1 guide RNA with the targeting sequence, GGTCCCTATGTAGCACGTTG, was used to generate MM1 crCdk5 cells. CrisprPDL1_G2 guide RNA with the targeting sequence, GACTTGTACGTGGTGGAGTA, was used to generate MM1 crPDL1 cells (*31*).

Western Blot Analysis

Primary antibodies to Cdk5, p35, IRF-1, IRF-2 (Santa Cruz Biotechnology, CA), IRF2BP2 (Abcam, Cambridge, MA), HRP secondary antibodies (Cell Signaling Technology, MA) were used for analysis. Whole cell lysates were prepared from mouse and human MB cell lines or other control cells by incubating 4×10^7 cells in 300 µl of lysis buffer (1% NP-40, 10mM Tris-HCl, pH7.5, 140mM NaCl, 2mM EDTA) supplemented with protease inhibitors (Roche), phosphatase inhibitor cocktails 1 and 2 (Sigma-Aldrich) and Na_2VO_3 for 30min on ice followed by centrifugation at 12,000x g for 20min at 4^{o}C to remove nuclei and other cell debris. Total protein concentration was determined using the BioRad DC protein assay kit (BioRad cat# 500-0116) and the

lysates were either used immediately or stored at –80°C. To generate immunoblots, samples were boiled for 5 min at 95°C in 4x LDS sample buffer containing β-ME, separated on 4-20% Tris-Glycine gels, and the proteins were subsequently transferred onto 0.2 μm nitrocellulose membranes. After blocking for 1 h at RT in 5% non-fat dry milk in 1x TBS/T 0.05%, blots were incubated overnight at 4°C in primary antibodies to detect target proteins. A blot incubated with anti-beta Actin served as a loading control. After washing (3x for 5min) in 1xTBS/T, the membranes were incubated for 2 h at RT with a 1:1000 dilution of relevant secondary antibodies followed by SuperSignal West Pico chemiluminescence and bands were visualized using ChemiDoc (BioRad, Inc.).

Flow Cytometric Analysis

Purified or fluorescently labeled antibodies against mouse H-2K^b (clone AF6-88.5), I-A^b (AF6-120.1), PD-1, (clone RMP1-14), PD-L1 (clone 1H5), PD-L2 (clone TY25), FAS-L (clone MFL3), CD80 (clone 16-10A1), CD86 (GL-1), and appropriate secondary antibodies were used as recommended by the manufacture. Briefly, 5×10^5 to 1×10^6 cells in 100 μl of FACS buffer were incubated staining or isotype-control antibodies on ice in the dark for 45min. After washing, cells were resuspended in 100 μl of FACS buffer and incubated with 7-AAD for 10 min for live/dead cell discrimination. Data were acquired immediately by Accuri or FACScaliber and analyzed by FlowJo.

Kinase Activity Assay

Cdk5-specific kinase activity assay was performed using luminescent kinase assay kit as per manufacturer's protocol with slight modifications (Promega). In brief, cell lysates were prepared at 1 μg/μl concentration and precleared with protein A-agarose beads and rabbit IgG (Santa Cruz Biotechnology) at 4°C for 2 h. An overnight incubation at 4°C with 5 μg of anti-Cdk5 IgG, followed by 3 h at 4°C with 25 μl of protein A-agarose beads, immunoprecipitated Cdk5 from the lysates. Immunoprecipitates were washed twice with lysis buffer and twice with kinase buffer [20 mM Tris·HCl (pH 7.4)/10 mM MgCl2/1 mM EDTA/10 μM NaF/1 μM Na2VO3] and resuspended in 30 μl of water. Ten microliters of kinase assay mixture [100 mM Tris·HCl (pH 7.4)/50 mM MgCl2/5 mM EDTA/50 μM NaF/5 μM Na2VO3/5 mM DTT] and 20 μM NF-H peptide in presence of ATP/ADP-glo mixture and luminescence was measured as readout of correlative kinase activity.

Quantitative PCR Assay

Total cellular RNA was isolated from 5×10^6 to 5×10^7 cells using TRIZOL and RNAspin Mini kit (GE Healthcare, UK), treated with DNAseI to eliminate genomic DNA, and quantitated using the NanoDrop2000 spectrophotometer. Reverse transcription (RT) of 1 μg of total RNA was performed with oligo(dT)16 using on using SuperScript First Strand Synthesis System for RT-PCR kit (Life Technologies, Carlsbad, CA). The resulting cDNA was used as a template for the amplification of target gene transcripts by real time PCR, using SYBR Green PCR Master Mix (Life Technologies, Carlsbad, CA) on the ABI 7300 Real-Time PCR machine (Life Technologies, Carlsbad, CA). Target gene expression was calculated using the standard curve method upon normalization to cytochrome c housekeeping gene. The primer sequences were as follows: Cdk5 forward: GTCCATCGACATGTGGTCAG; Cdk5 reverse: CTGGTCATCCACATCATTGC;

cytochrome c forward: CTGCCACAGCATGGATTATG; cytochrome c reverse: CATCATCATTAGGGCCATCC; p35 forward: GTCCCTATCCCCCAGCTATC; p35 reverse: TTCTTGTCCTTGGCGTTCTT; PD-L1 forward: TGCTGCATAATCAGCTACGG and PD-L1 reverse: TCCACGGAAATTCTCTGGTT.

Genomic Analysis Using Online Data sets

Cdk5, p35, and p39 mRNA expression was analyzed in pediatric MB and neuroblastoma (NB) samples from the publicly available "Pediatric Tumor Affymetrix Database" of Dr. Javed Khan (Version 2013-09-27; http://pob.abcc.ncifcrf.gov/cgi-bin/JK) accessed through the University of California Santa Cruz Cancer Genomics Browser (https://genome-cancer.ucsc.edu/) (*35*). Publicly available data sets from The Cancer Genome Atlas (TCGA) including numerous cancer types were accessed from the public access data portal of the Memorial Sloan Kettering Cancer Center cBioPortal (www.cbioportal.org/) (*36*) and analyzed for Cdk5 and PD-L1 (CD274) mRNA expression and mutual exclusivity or co-occurrence of upregulated transcript levels. The results shown are based in part upon data generated through the TCGA Research Network: https://tcga-data.nci.nih.gov/tcga/. Using the PrognoScan database (www.prognoscan.org/) and publicly available Gene Expression Omnibus (www.ncbi.nlm.nih.gov/geo) data sets with the accession numbers GSE 4412-GPL96, GSE19234, GSE22138, GSE68485, GSE4922-GPL96, or the publicly available MGH-glioma data set from the Broad Institute (www.broadinstitute.org/cgi-bin/cancer/datasets.cgi), the relationship between Cdk5 expression levels and overall, disease free, or distant metastasis free survival rates were evaluated in glioma, melanoma, breast and lung cancer patients. Patients were stratified into two groups according to their intratumoral Cdk5 expression at various cutoffs, and the cutoff point yielding the most significant survival difference by log-rank test is presented in the Kaplan Meier analysis.

Treatment of MB Cell Lines with Recombinant Mouse IFN-γ (rmIFN-γ)

Murine MB cell lines MM1 WT, MM1 shCdk5 and MM1 shNS were grown in RPMI supplemented with 10% FBS. Once 80% confluent, culture medium was replaced with medium containing 100ng/ml rmIFN-γ (R&D Systems). Cells were incubated at 37^{o}C and harvested by incubating for 5min at 37^{o}C in 10mM EDTA/PBS at different time points (0 h, 4 h, 8 h and 24 h). In all subsequent experiments, treatment of cells was carried out for 24 h with 100ng/ml rmIFN-γ.

Treatment of MB Cell Lines with Roscovitine

Murine MB cell lines MM1 were grown in RPMI supplemented with 10% FBS. A stock solution of Roscovitine (10mM) or vehicle control-DMSO was diluted in fresh tumor medium and added to samples to achieve a final concentration of 10 μM or 20 μM. After 4 days of treatment, cells were subjected to 100ng/ml rmIFN-γ (R&D Systems) for 24 hours and then harvested for qPCR analysis.

Tumor Cell Preparation and Injection

For in vivo studies, 5 × 10^4 MM1 WT, MM1 shCdk5, or MM1 shNS cells were inoculated s.c. into the left thighs of C57BL/6J or B6 nude mice (B6.Cg/NTac-*Foxn1*^{nu} NE10). Mice were observed regularly for tumor presence by visual inspection

and manual palpation. Tumors were measured using an electronic caliper in the long and short dimensions, and tumor volumes were estimated using the equation: $V = \pi \cdot D \cdot d^2$, where D = long dimension and d = short dimension. The mice were typically sacrificed around days 21-28, and the tumor tissues were harvested for weight measurement and further tissue analyses.

IHC Staining

Following approval by University Hospitals Case Medical Center Institutional Review Board, human tissue microarrays were constructed from formalin-fixed and paraffin embedded samples of 6 human MB (4 males, 2 females; age 4-24; classic (2), nodular/desmoplastic (3) and large cell (1) variants), containing 3 cores (2 mm-diameter each) per case, and consecutive sections were stained with anti-human Cdk5 (clone 40773, Abcam) and anti-human CD3 (clone 2GV6, Ventana). Expression of Cdk5 was assessed semi-quantitatively on a 4-tiered scale as absent, weak, moderate, and strong; the total number of intratumoral $CD3^+$ lymphocytes was counted in 4-5 high-power fields (HPF) and presented as average number of lymphocytes per HPF. For murine samples, 5×10^4 MM1 shCdk5 or MM1 shNS cells were inoculated into the left thighs or i.c. of C57BL/6 mice. Tumor outgrowths were harvested 2 weeks later, and $CD3^+$ T cell infiltration was assessed by staining with anti-CD3 antibody (clone SP7, Abcam). PD-L1 expression was assessed on serial sections using anti-PD-L1 antibody (clone 28-8, Abcam).

In vivo Depletion of $CD4^+$ and $CD8^+$ T cells

To interrogate the role of different T cell subsets in rejecting Cdk5-deficient tumors, we conducted *in vivo* depletion of T cells in mice prior to and following Cdk5-deficient tumor inoculation. Different groups of mice were injected with 100ug of anti-CD4 antibody (GK1.5), anti-CD8 antibody (2.43) or both antibodies 72 h and 24 h prior to tumor inoculation and twice weekly thereafter to ensure sustained depletion of T cell subset depletion during the experimental period. One group of mice injected with IgG isotype served as controls. All mice were monitored for development of tumors up to day 42.

Phosphoproteomics

Phosphorylation sites were identified based on unbiased phosphopeptide enrichment workflow that couples the immunoprecipitation of phosphorylated peptides with LC-MS peak volume quantification. Global phosphorylation studies were performed in MM1 WT cells or MM1 cells with shCdk5 and shNS or crCdk5 and crNeg using an unfractionated label free approach. Analysis was run on 3 biologic repeats of each cell line. Cells were lysed in a 2% SDS solution with protease (P845, Sigma Aldrich) and phosphatase (PhosphoSTOP, Roche) inhibitors. Two hundred microliters of cell lysate was washed using the FASP cleaning procedure to remove detergent. All cells were digested with a 2-step Lys C/Trypsin proteolytic cleavage. Samples were then enriched for phosphorylation using TiO2 enrichment spin tips (Thermo Fisher), and subjected to LC-MS/MS using a UPLC system (NanoAcquity) interfaced with an Orbitrap ProVelos Elite MS (Thermo Fisher) for data collection. Rosetta Elucidator software was used to cluster all peptide precursor ions and downstream quantitative modules were used to

quantify phosphopeptides. The MASCOT (Matrix Science) protein database was used to identify peptides and proteins. Phosphopeptides with greater than a ± 2-fold change were identified and subjected to One-Way ANOVA analysis to determine statistical significance ($p < 0.02$). Peptides where analyzed with either Ingenuity Pathway Analysis and/or Microsoft Excel.

Statistical Analysis

Statistical analyses were performed using GraphPad Prism 5 and 6 software (GraphPad Software Inc, San Diego, CA). To test for statistical significance, the *t* test (Fig. 2C, 4B-H, S3B, S3D, S9A, S9C-I), and two-way analysis of variance with Bonferonni (Fig. 2A, 2B) or Tukey's (S4D, S4E) posttests were used to compare between treatment groups. For survival curves log-rank test was used to compare between individual groups (Fig. 2G, 3A, 3B, 3D, S3A, S3C, S3E). For all analyses $P < 0.05$ was considered significant. Results are collective data from 3 to 10 repeat experiments with minimum of 3 mice per experiment.

Supplementary Text

Author Contributions

A.P., R.D.D. and A.Y.H. conceived the experiments. A.P., R.D.D., J.N., J.T.M., S.M.C., T.P., D.W.A., S.A., J.J.L., D.S. and A.Y.H. executed the experiments and analyzed the data. All authors contributed to writing the manuscript.

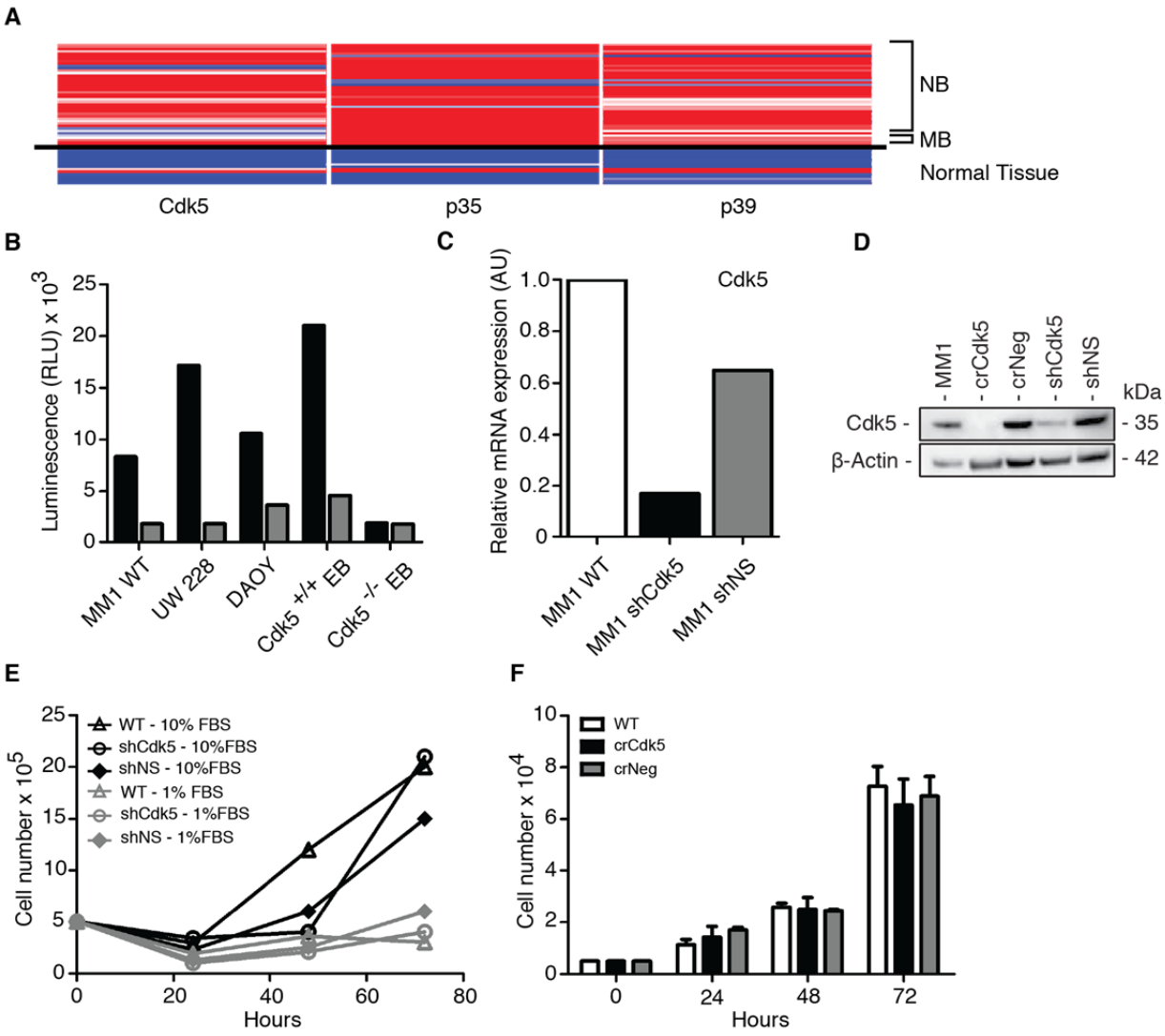

Fig S1. Kinase active Cdk5 is expressed by murine and human MB cell lines and deletion of Cdk5 does not alter proliferation. (A) Genomic analysis from the UCSC cancer genome browser demonstrates that Cdk5, p35, and p39 are highly expressed in pediatric MB (4 patients) and neuroblastoma (NB) (39 patients) samples (above black line) compared to normal brain tissue (below black line). **(B)** Cdk5 kinase assay activity is detected in human MB (UW228, DAOY) and mouse MB (MM1) cell lines, with lysates from $Cdk5^{-/-}$ and $Cdk5^{+/+}$ embryonic brains as negative and positive controls, respectively (Black Bars). The non-selective Cdk5 inhibitor, Roscovitine (10 μM), abrogates this kinase activity (Gray bars). **(C)** mRNA expression of Cdk5 transcript in MM1 WT (white), shCdk5 (black), or shNS (gray). **(D)** MM1 shCdk5 and MM1 crCdk5 are deficient in Cdk5 protein expression. **(E)** Proliferation curves of MM1 WT (square), shCdk5 (triangle), and shNS (circle) in media with 10% serum (black lines) or 1% serum (gray lines) over 72 hours **(F)** Proliferation curves of MM1 WT (white), crCdk5 (black), crNeg (gray) in media containing 10% serum over 72 hours. Data represent mean ±SD from biologic triplicates.

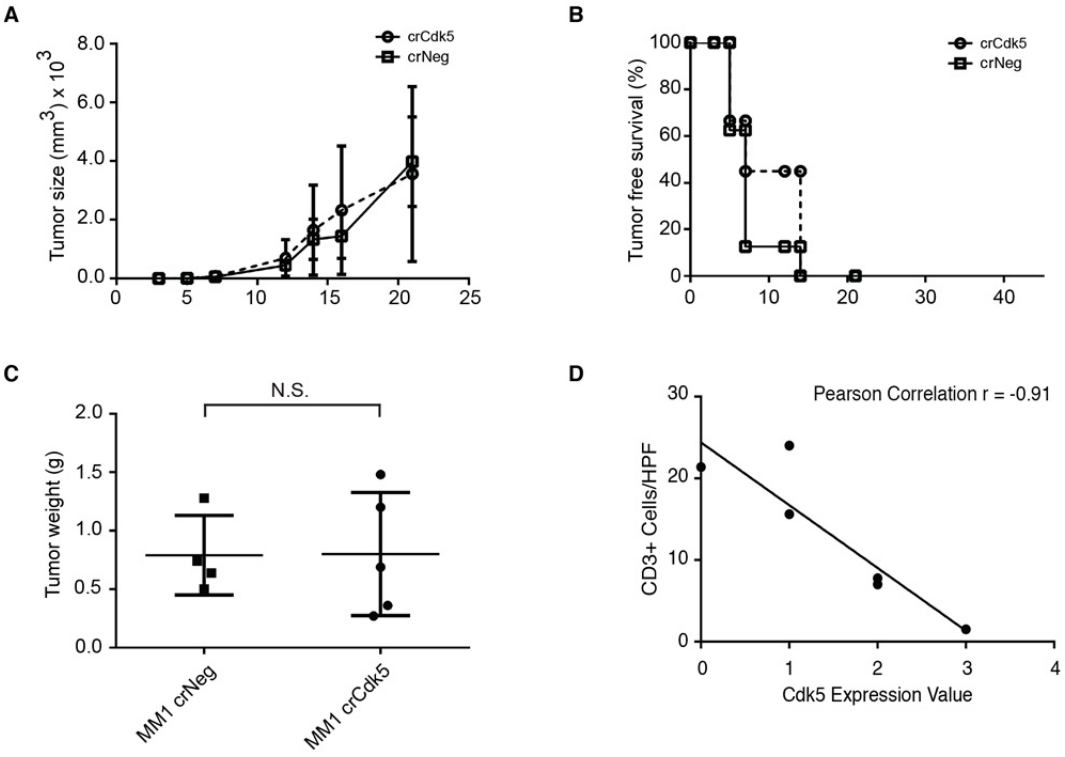

Fig S2. Similar subcutaneous (s.c.) growth kinetics of crCdk5 MM1 and crNeg MM1 in immune-compromised mice. (A) *In vivo,* growth kinetics of MM1 crCdk5 (circle) and crNeg (square) in NSG mice (n = 10/group). Points were graphed as the average size ± SD. **(B)** TFS of MM1 crCdk5 (circle) and crNeg (square) in NSG mice. **(C)** Tumor weights of MM1 crCdk5 (circle) and crNeg (square) in NSG mice. The solid line represents the average weight ± SD. **(D)** Inverse correlation between $CD3^+$ cell count per HPF and Cdk5 staining intensity of clinical MB tissue samples as revealed by IHC analysis in Fig. 1D. Significance was determined using a t test (C).

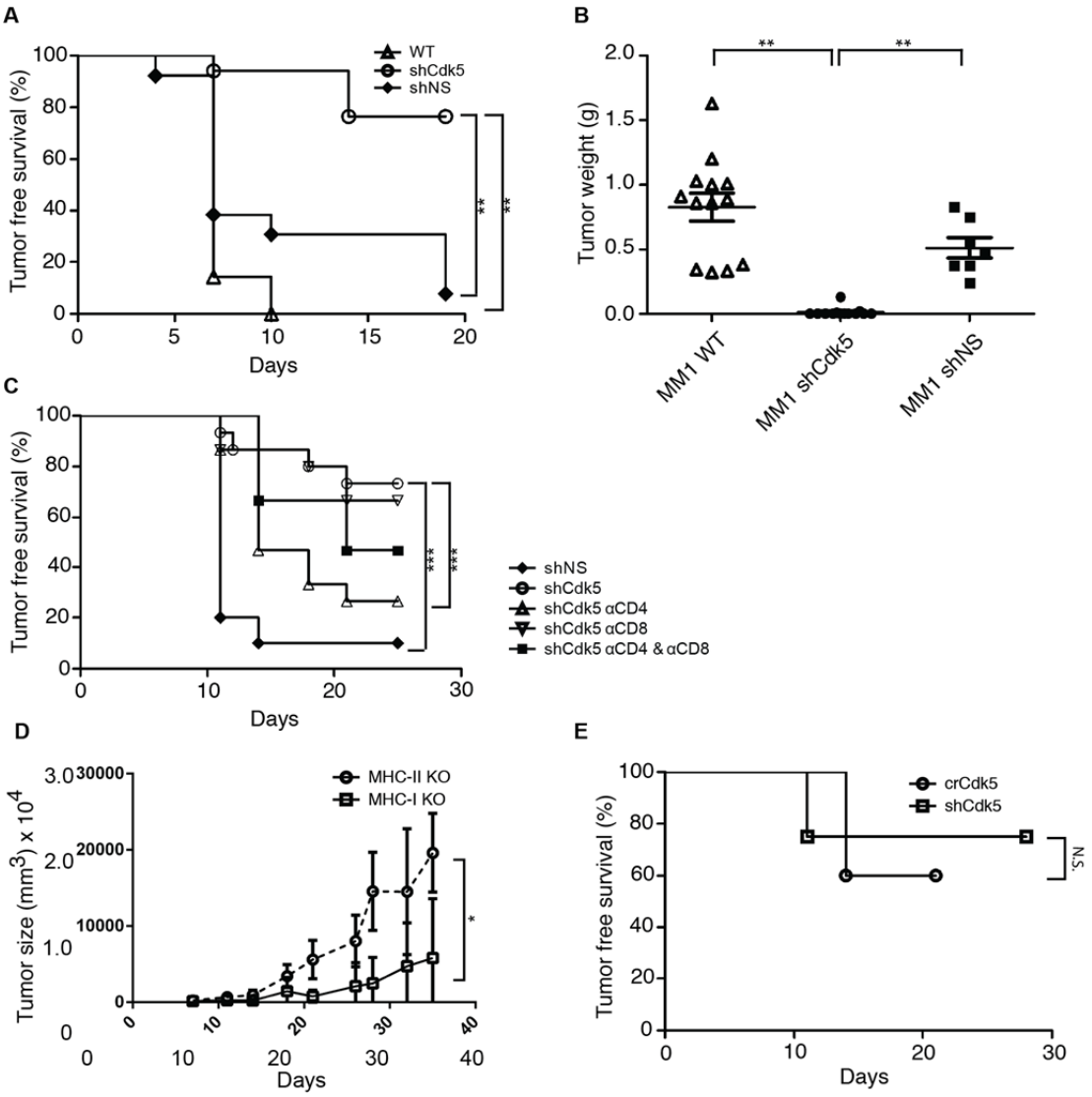

Fig S3. ***In vivo*** **growth kinetics of MM1 shCdk5 reveals thymic dependent tumor rejection upon s.c. injection. (A)** TFS of MM1 WT (diamond, *n* = 13), shCdk5 (circle, *n* = 17), and shNS in B6 mice (triangle, *n* = 7). Survival curves were calculated from 3 independent experiments. **(B)** Tumor weights of MM1 WT (triangles, *n* = 13) and shCdk5 (circles, *n* = 13) and shNS (squares, *n* = 7). The solid line represents the average weight ± SD. **(C)** TFS of B6 mice injected s.c. with MM1 shNS (diamond, *n* = 10) or MM1 shCdk5 (circle) with injection of αCD4 (triangle), αCD8 (inverted triangle), or αCD4 and αCD8 (square) antibodies (*n* = 15/group). **(D)** Tumor size measurement of MHC-II KO (circle) and MHC-I KO (square) mice injected s.c. with Cdk5-deficient MM1 (*n* = 10/group). **(E)** TFS of B6 mice re-challenged with MM1 WT at least 60 days post-initial injection of MM1 shCdk5 (square) or MM1 crCdk5 (circle) (*n* = 5/group). **P < 0.01; ***P < 0.001 Significance was determined by log rank test (A, C, E) or *t* test (B, D).

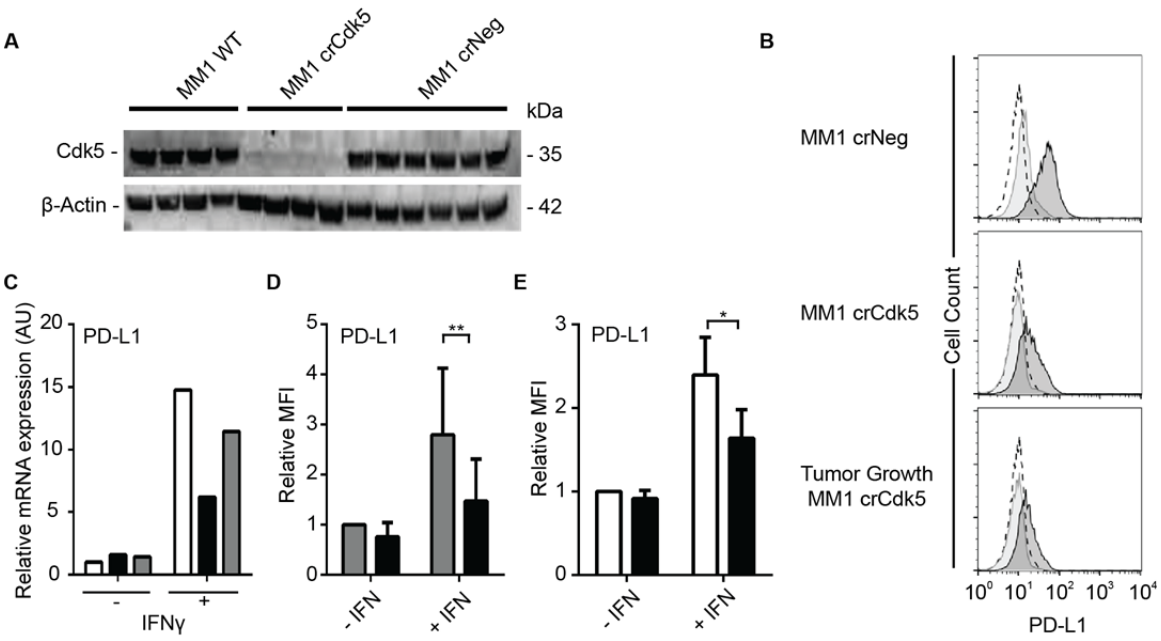

Fig S4. A link between Cdk5 and PD-L1 expressions in human and murine tumors. **(A)** Cdk5 expression of cells cultured from subcutaneous tumor outgrowths isolated from animals initially injected with MM1 WT (n = 4), crCdk5 (n = 4), or crNeg (n = 6). **(B)** PD-L1 expression on primary cell cultures of MM1 crNeg, crCdk5, or outgrowth of crCdk5 tumors. Cells were stimulated with IFNγ for 24 hours (black) and compared to isotype staining (dotted line) and un-stimulated cells (gray). Histogram is a representative staining from three separate experiments. **(C)** PD-L1 mRNA expression by RMS 76.9 WT (white), shCdk5 (black), and shNS (gray) with or without 24 hours of IFNγ stimulation. **(D)** Surface PD-L1 staining of RMS 76.9 shNS (gray) and shCdk5 (black) with or without 24 hours of IFNγ stimulation. Values represent the average MFI ± SD compared to unstimulated RMS 76.9 shNS over three independent experiments. **(E)** Surface PD-L1 staining of SJCRH30 WT (white) and crCdk5 (black) with or without 24 hours of IFNγ stimulation *in vitro*. Values represent average MFI ± SD compared to unstimulated WT over three independent experiments. *P<0.05; **P<0.005. Significance was determined by two-way analysis of variance (ANOVA) (D) and (E).

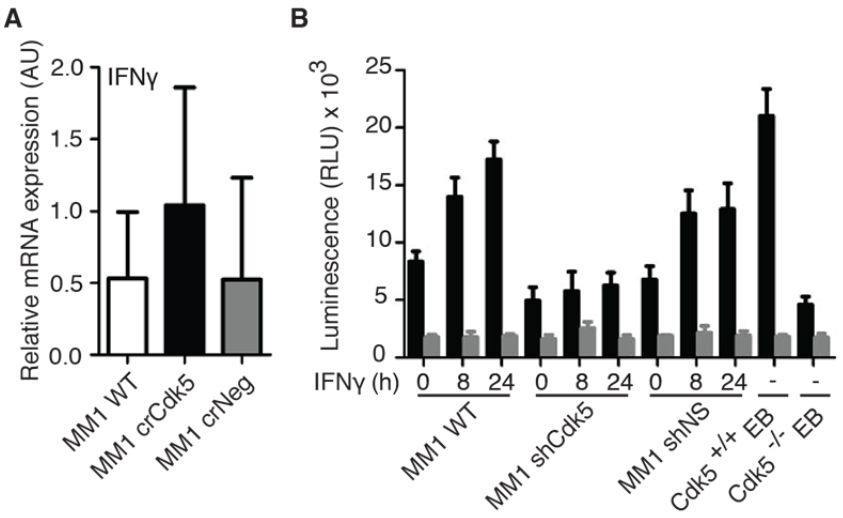

Fig S5. Disruption of Cdk5 gene expression results in more IFNγ in the tumor bed and decreased Cdk5 activity in response to IFNγ. (A) *In vivo* IFNγ mRNA expression in tumor extracts from i.c. inoculations (*n* = 3 mice/group; ± SD). **(B)** Cdk5 kinase activity in MM1 WT, shCdk5, and shNS over the course of 24-hour stimulation with IFNγ (black) and the addition of 10 μM Roscovitine (gray). EB: embryonic brain.

A

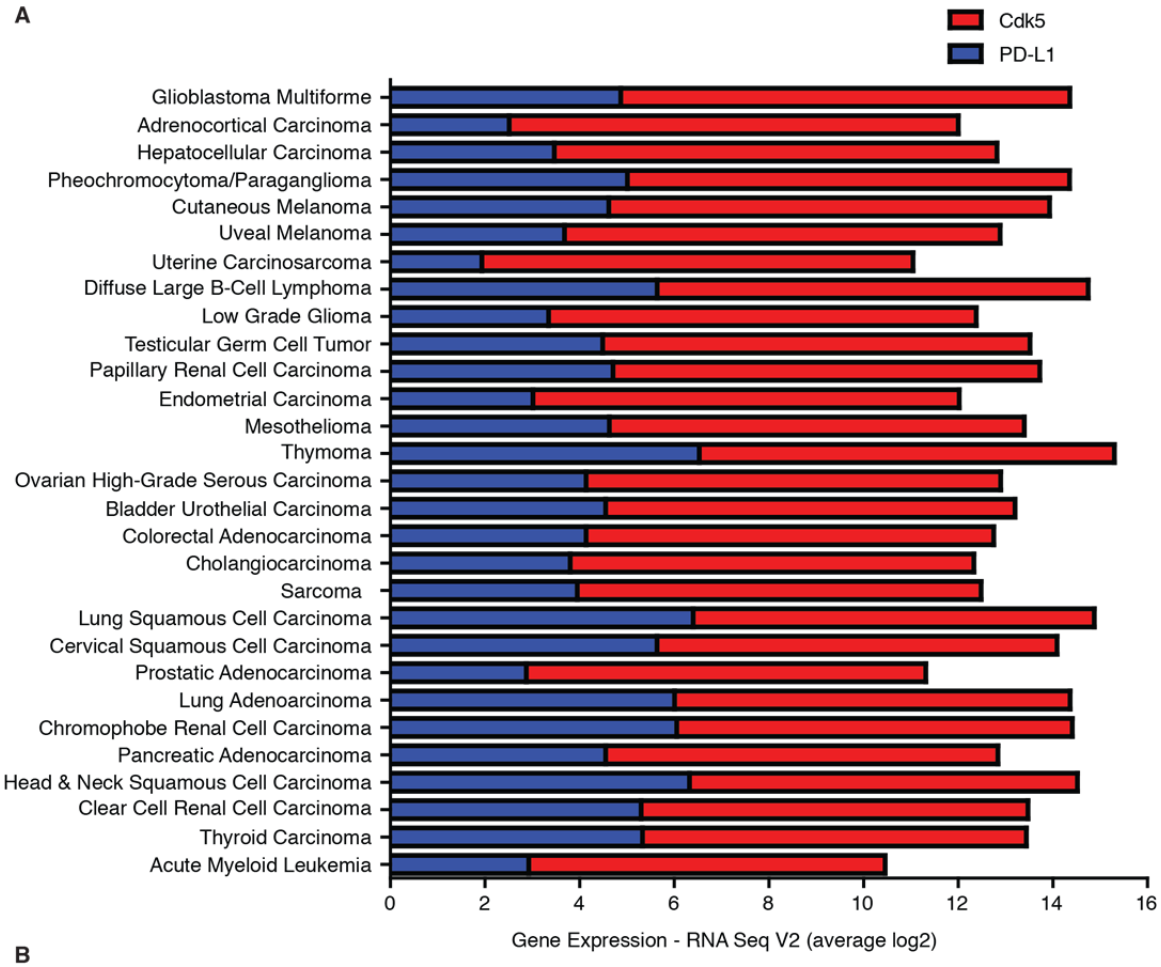

B

Cdk5 & PD-L1 mRNA expression analysis:	p-value	log odds Ratio	Association
Lung Adenocarcinoma (TCGA, Provisional)	0.001	2.138	Co-occurrence
Papillary Thyroid Carcinoma (Cell, 2013)	0.06	1.018	Co-occurrence
Thyroid (TCGA, Provisional)	0.067	0.977	Co-occurrence
Lymphoid Neoplasm Diffuse Large Cell B-Cell Lymphoma (TCGA, Provisional)	0.071	>3	Co-occurrence
Breast Invasive Carcinoma (TCGA, Provisional)	0.289	0.437	Co-occurrence
Glioblastoma Multiforme (TCGA, Cell 2013)	0.311	1.128	Co-occurrence
Uterine Corpus Endometrial (TCGA, Provisional)	0.382	0.916	Co-occurrence
Liver Hepatocellular Carcinoma (TCGA, Provisional)	0.628	0.094	Co-occurrence

Fig S6. Co-occurrence of upregulated Cdk5 and PD-L1 expression in human cancer samples. TCGA provisional data sets for all available cancer types were analyzed for Cdk5 and PD-L1 (CD274) mRNA expression through cBioPortal (http://www.cbioportal.org/). **(A)** Relative mRNA expression values of samples with existing RNA sequencing analysis (RNA Seq V2) were downloaded and analyzed with microsoft excel. The average log2 mRNA expression across each cancer type examined was individually graphed for Cdk5 and PD-L1. **(B)** Co-occurrence of elevated Cdk5 and PD-L1 gene expression is observed in several cancer types. mRNA expression z-scores of RNA Seq V2 RSEM from available tumors were analyzed for significance, their log odds ratio, and type of association. Representative cancer types showing co-occurrence of elevated Cdk5 and PD-L1 transcript levels are displayed.

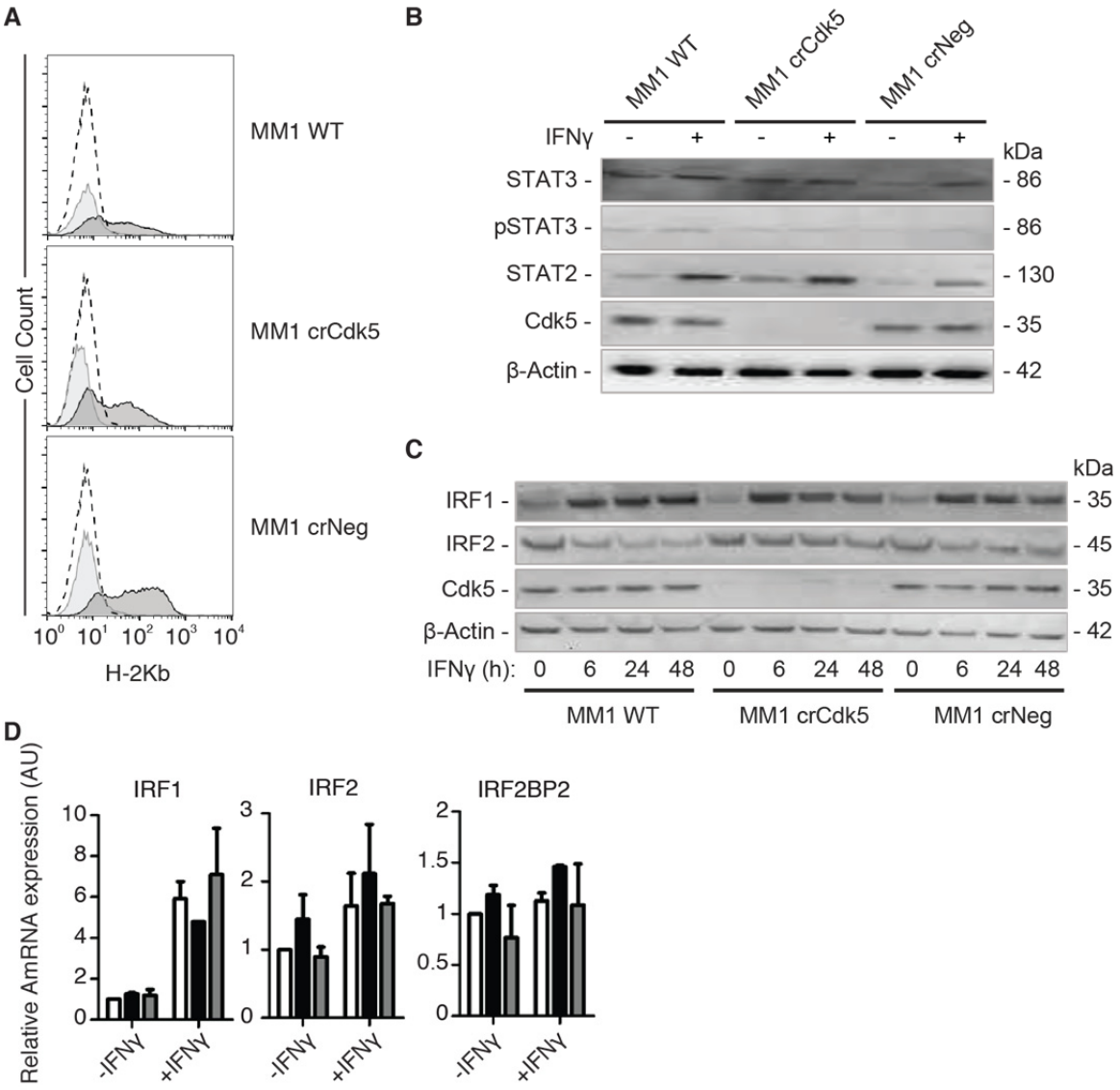

Fig S7. Silencing Cdk5 in MB alters IRF-2 expression but does not affect other IFN signaling pathways. (A) Surface expression of MHC-I is upregulated on MM1 WT, crCdk5, and crNeg. Cells were stimulated with IFNγ for 24 hours (black) and compared to isotype staining (dotted line) and unstimulated cells (gray). Histogram is a representative staining from three separate experiments. **(B)** 24-hour stimulation of MM1 WT, crCdk5, and crNeg cells. Downstream IFNγ pathway elements STAT3, phosphorylated (p)STAT3, and STAT2 were assayed. **(C)** IFNγ stimulation of MM1 WT, crCdk5, and crNeg over the course of 48 hours. IFNγR downstream mediators IRF1, and IRF2 were assayed. **(D)** *In vitro* mRNA analysis of *IRF-1*, *IRF-2*, and *IRF2BP2* present in MM1 WT (white), crCdk5 (black), and crNeg (gray) after treatment with IFNγ for 24 hours. Significance was determined using a 2-Way ANOVA (D).

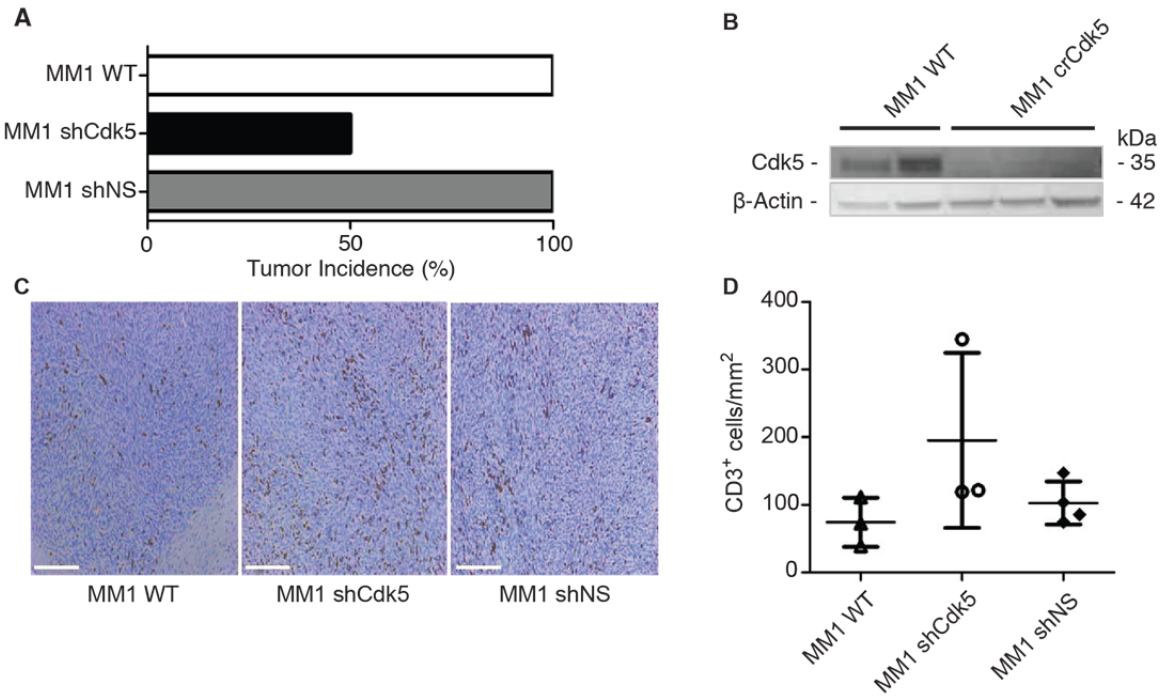

Fig S8. CD3$^+$ cell infiltrate and diminished growth rates associate with a decrease in tumor incidence following orthotopic administration of Cdk5-deficient MM1 cells. **(A)** Tumor incidence of MM1 WT, shCdk5, and shNS 14 days after i.c. tumor inoculation. **(B)** Western blot analysis for Cdk5 in cells cultured from B6 mice tumor outgrowths initially inoculated with MM1 WT (n = 2) and MM1 crCdk5 (n = 3). **(C)** IHC of tumor injected i.c. with MM1 WT, shCdk5, and shNS (scale bar = 200 μm). **(D)** Quantification of intratumoral CD3$^+$ cells in MM1 WT (n = 3), shCdk5 (n = 3), and shNS (n = 4) tumors identified via IHC per mm^2 of tumor tissue. Solid line represents the average ± SD. Significance was determined using a Student's t test (D).

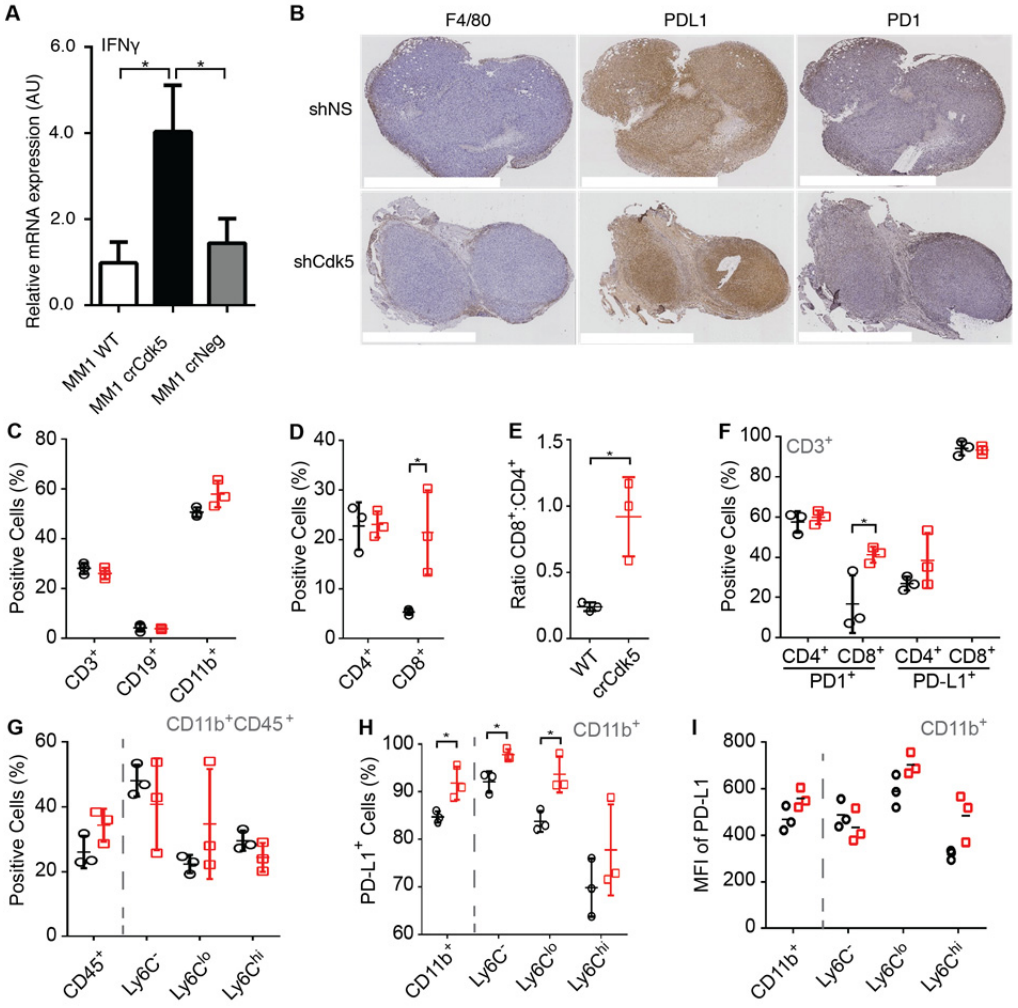

Fig S9. Subcutaneous Cdk5 deficient tumors characterized by increased stromal PD-L1 staining, CD4$^+$ tumor infiltrating lymphocytes (TIL), and infiltrating CD11b$^+$ populations. (A) *In vivo* IFNγ mRNA expression in tumor extracts from subcutaneous inoculations (n = 3 mice/group; ± SD). **(B)** S.c. tumors extracted 14 days post-inoculation from MM1 shCdk5 or shNS stained for F4/80, PD-L1, and PD-1 expression (Scale bars = 2mm). **(C), (D)** FACS analysis of MM1 WT (black circle) and MM1 crCdk5 (red square) tumor infiltrate by percentage of cell type. **(E)** Ratio of total CD8$^+$:CD4$^+$ cell infiltrate. **(F)** FACS analysis of the percentage of PD-1$^+$ or PD-L1$^+$ cells in the CD4$^+$ or CD8$^+$ populations. **(G)** FACS analysis of the percentage of myeloid cells in tumor infiltrate based on differential CD45 staining (left) or Ly6C staining among CD11b$^+$CD45$^+$ cells (right). **(H)** Percent of total CD11b$^+$ population (left) and sub-populations (right) present in tumor infiltrate that express PD-L1. **(I)** MFI of PD-L1 expression between total (left) and sub-populations (right) of CD11b$^+$ cells. **C** thru **H** were graphed as the mean ± SD. **(I)** was graphed as individual MFI with mean indicated. n = 9/group. Each data point represents pooled samples from 3 mice. *P < 0.05 Significance was determined by Student's t test.

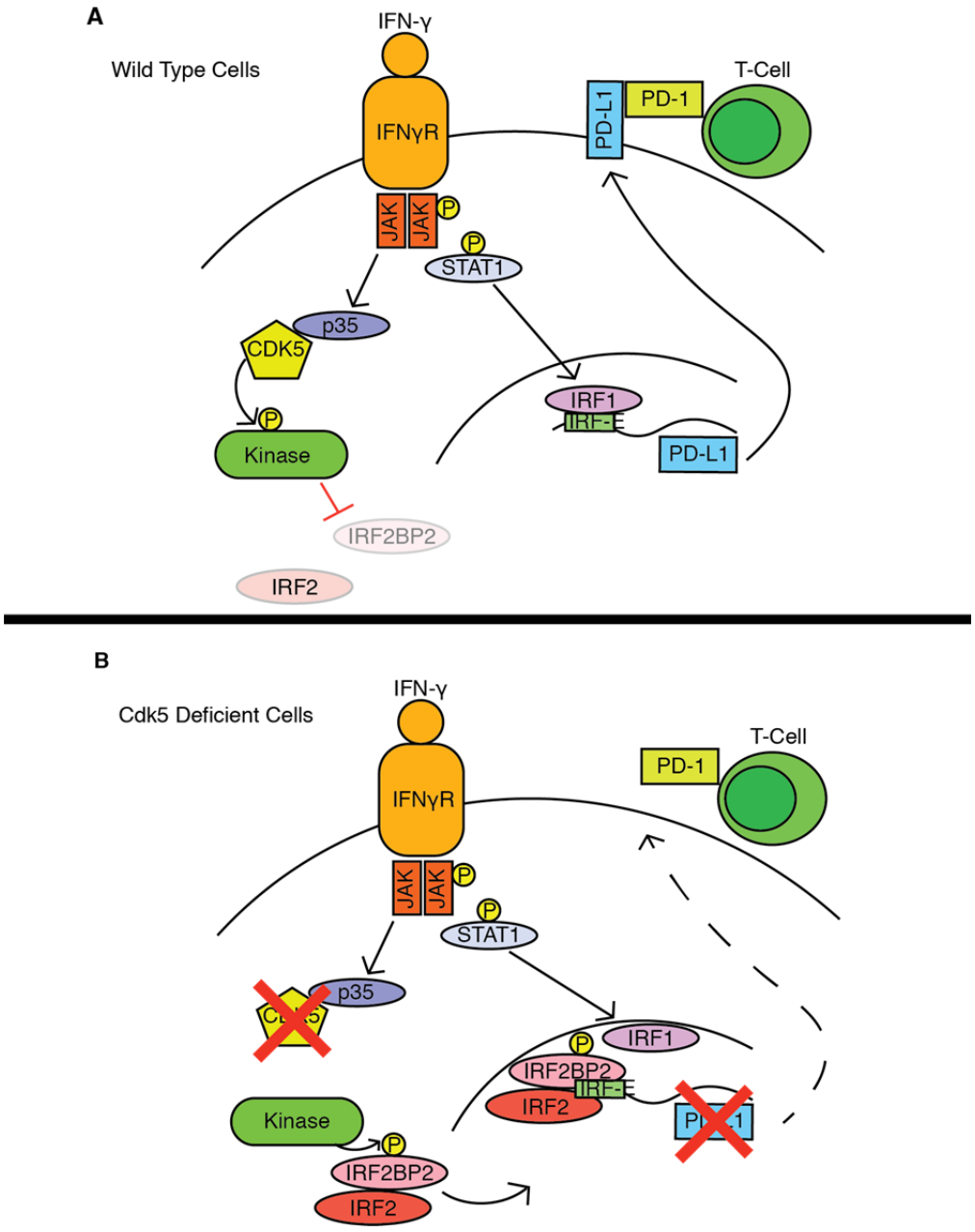

Fig S10. Putative mechanism by which Cdk5 controls PD-L1 expression. (A) When Cdk5 WT cells are stimulated with IFNγ, signaling through the JAK/STAT pathway stimulates IRF-1 driven transcription of PD-L1. Additionally, IFNγ stimulates p35 expression and thereby increases Cdk5 activity. Phosphorylation of unknown kinase(s) by Cdk5 inhibits kinase function, resulting in a reduced abundance of the IRF2/IRF2BP2 repressor complex. **(B)** In Cdk5 deficient cells, unknown kinase(s) hyper-phosphorylate IRF2BP2, prolong half-life of IRF2/IRF2BP2 repressor complex despite intact JAK/STAT/IRF-1 signaling, ultimately leading to decreased PD-L1 expression. IRF-E: IRF-binding element.

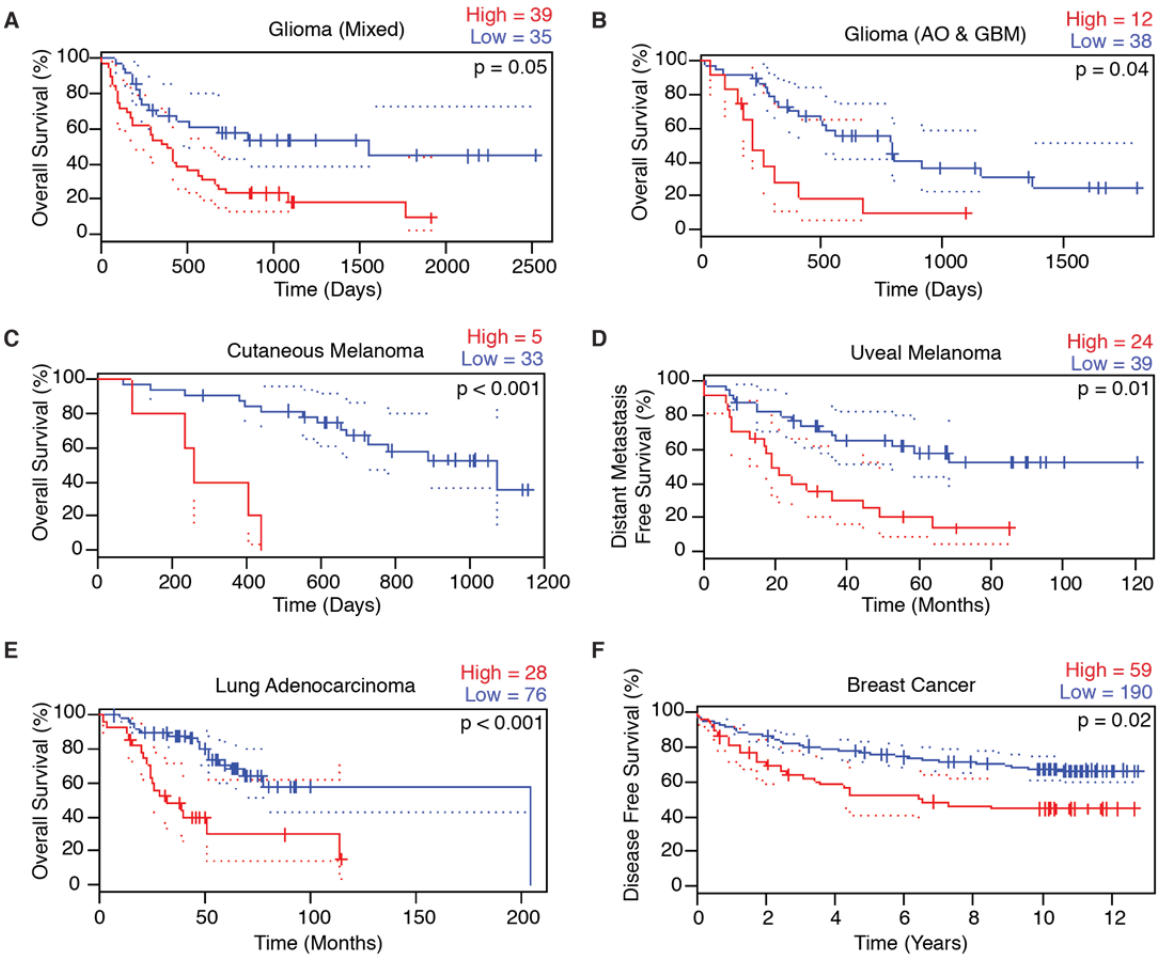

Fig. S11 Higher Cdk5 correlates with adverse clinical outcomes in human cancers. PrognoScan database-based Kaplan-Meier analysis of six independent patient cohorts including CNS and peripheral tumors that were analyzed for the effects of higher levels of Cdk5 gene expression (red) compared to low Cdk5 levels (blue) on overall survival, disease free survival, or metastasis free survival (http://www.prognoscan.org/). High levels of Cdk5 are associated with reduced **(A)** overall survival in a cohort of 74 glioma patients with astrocytoma (n = 8), GBM (n = 50), mixed glioma (n = 7), and oligodendroglioma (n = 9) (GSE 4412-GPL96); **(B)** overall survival in 50 patients with anaplastic oligodendroglioma (n = 22) and GBM (n = 28) (MGH-glioma); **(C)** overall survival of cutaneous melanoma patients (n = 38) (GSE19234); **(D)** distant metastasis free survival in uveal melanoma patients (n = 63) (GSE22138); **(E)** overall survival in a cohort of 104 patients with lung adenocarcinoma (GSE68465); and **(F)** disease free survival in a cohort of 249 breast cancer patients (GSE4922-GPL96). All p-values represent the corrected p-value.

Excel tables

Table S1. shCdk5-All phosphoproteomics data
Table S2. shCdk5-Significant phosphoproteomics data
Table S3. crCdk5-All phosphoproteomics data
Table S4. crCdk5-Significant phosphoproteomics data

References and Notes

1. R. Dhavan, L. H. Tsai, A decade of CDK5. *Nat. Rev. Mol. Cell Biol.* **2**, 749–759 (2001). Medline doi:10.1038/35096019

2. T. Ohshima, J. M. Ward, C. G. Huh, G. Longenecker, H. C. Veeranna, R. O. Pant, L. J. Brady, A. B. Martin, A. B. Kulkarni, Targeted disruption of the cyclin-dependent kinase 5 gene results in abnormal corticogenesis, neuronal pathology and perinatal death. *Proc. Natl. Acad. Sci. U.S.A.* **93**, 11173–11178 (1996). Medline doi:10.1073/pnas.93.20.11173

3. E. Utreras, A. Futatsugi, T. K. Pareek, A. B. Kulkarni, Molecular roles of Cdk5 in pain signaling. *Drug Discov. Today Ther. Strateg.* **6**, 105–111 (2009). Medline doi:10.1016/j.ddstr.2009.04.004

4. E. Contreras-Vallejos, E. Utreras, C. Gonzalez-Billault, Going out of the brain: Non-nervous system physiological and pathological functions of Cdk5. *Cell. Signal.* **24**, 44–52 (2012). Medline doi:10.1016/j.cellsig.2011.08.022

5. A. Arif, Extraneuronal activities and regulatory mechanisms of the atypical cyclin-dependent kinase Cdk5. *Biochem. Pharmacol.* **84**, 985–993 (2012). Medline doi:10.1016/j.bcp.2012.06.027

6. T. K. Pareek, E. Lam, X. Zheng, D. Askew, A. B. Kulkarni, M. R. Chance, A. Y. Huang, K. R. Cooke, J. J. Letterio, Cyclin-dependent kinase 5 activity is required for T cell activation and induction of experimental autoimmune encephalomyelitis. *J. Exp. Med.* **207**, 2507–2519 (2010). Medline doi:10.1084/jem.20100876

7. F. N. Hsu, M. C. Chen, M. C. Chiang, E. Lin, Y. T. Lee, P. H. Huang, G. S. Lee, H. Lin, Regulation of androgen receptor and prostate cancer growth by cyclin-dependent kinase 5. *J. Biol. Chem.* **286**, 33141–33149 (2011). Medline doi:10.1074/jbc.M111.252080

8. G. Feldmann, A. Mishra, S. M. Hong, S. Bisht, C. J. Strock, D. W. Ball, M. Goggins, A. Maitra, B. D. Nelkin, Inhibiting the cyclin-dependent kinase CDK5 blocks pancreatic cancer formation and progression through the suppression of Ras-Ral signaling. *Cancer Res.* **70**, 4460–4469 (2010). Medline doi:10.1158/0008-5472.CAN-09-1107

9. R. Liu, B. Tian, M. Gearing, S. Hunter, K. Ye, Z. Mao, Cdk5-mediated regulation of the PIKE-A-Akt pathway and glioblastoma cell invasion. *Proc. Natl. Acad. Sci. U.S.A.* **105**, 7570–7575 (2008). Medline doi:10.1073/pnas.0712306105

10. H. S. Khalil, V. Mitev, T. Vlaykova, L. Cavicchi, N. Zhelev, Discovery and development of Seliciclib. How systems biology approaches can lead to better drug performance. *J. Biotechnol.* **202**, 40–49 (2015). Medline doi:10.1016/j.jbiotec.2015.02.032

11. H. J. Kim, H. Cantor, CD4 T-cell subsets and tumor immunity: The helpful and the not-so-helpful. *Cancer Immunol. Res.* **2**, 91–98 (2014). Medline doi:10.1158/2326-6066.CIR-13-0216

12. J. H. Song, C. X. Wang, D. K. Song, P. Wang, A. Shuaib, C. Hao, Interferon gamma induces neurite outgrowth by up-regulation of p35 neuron-specific cyclin-dependent kinase 5 activator via activation of ERK1/2 pathway. *J. Biol. Chem.* **280**, 12896–12901 (2005). Medline doi:10.1074/jbc.M412139200

13. S. J. Lee, B. C. Jang, S. W. Lee, Y. I. Yang, S. I. Suh, Y. M. Park, S. Oh, J. G. Shin, S. Yao, L. Chen, I. H. Choi, Interferon regulatory factor-1 is prerequisite to the constitutive expression and IFN-gamma-induced upregulation of B7-H1 (CD274). *FEBS Lett.* **580**, 755–762 (2006). Medline doi:10.1016/j.febslet.2005.12.093

14. J. M. Taube, R. A. Anders, G. D. Young, H. Xu, R. Sharma, T. L. McMiller, S. Chen, A. P. Klein, D. M. Pardoll, S. L. Topalian, L. Chen, Colocalization of inflammatory response with B7-h1 expression in human melanocytic lesions supports an adaptive resistance mechanism of immune escape. *Sci. Transl. Med.* **4**, 27ra37 (2012). Medline

15. H. Harada, T. Fujita, M. Miyamoto, Y. Kimura, M. Maruyama, A. Furia, T. Miyata, T. Taniguchi, Structurally similar but functionally distinct factors, IRF-1 and IRF-2, bind to the same regulatory elements of IFN and IFN-inducible genes. *Cell* **58**, 729–739 (1989). Medline doi:10.1016/0092-8674(89)90107-4

16. K. S. Childs, S. Goodbourn, Identification of novel co-repressor molecules for Interferon Regulatory Factor-2. *Nucleic Acids Res.* **31**, 3016–3026 (2003). Medline doi:10.1093/nar/gkg431

17. C. D. Pham, C. Flores, C. Yang, E. M. Pinheiro, J. H. Yearley, E. J. Sayour, Y. Pei, C. Moore, R. E. McLendon, J. Huang, J. H. Sampson, R. Wechsler-Reya, D. A. Mitchell, Differential immune microenvironments and response to immune checkpoint blockade among molecular subtypes of murine medulloblastoma. *Clin. Cancer Res.* **22**, 582–595 (2016). Medline doi:10.1158/1078-0432.CCR-15-0713

18. L. C. Platanias, Mechanisms of type-I- and type-II-interferon-mediated signalling. *Nat. Rev. Immunol.* **5**, 375–386 (2005). Medline doi:10.1038/nri1604

19. S. Yao, L. Jiang, E. K. Moser, L. B. Jewett, J. Wright, J. Du, B. Zhou, S. D. Davis, N. L. Krupp, T. J. Braciale, J. Sun, Control of pathogenic effector T-cell activities *in situ* by PD-L1 expression on respiratory inflammatory dendritic cells during respiratory syncytial virus infection. *Mucosal Immunol.* **8**, 746–759 (2015). Medline doi:10.1038/mi.2014.106

20. T. Taniguchi, A. Takaoka, A weak signal for strong responses: interferon-alpha/beta revisited. *Nat. Rev. Mol. Cell Biol.* **2**, 378–386 (2001). Medline doi:10.1038/35073080

21. H. Soliman, F. Khalil, S. Antonia, PD-L1 expression is increased in a subset of basal type breast cancer cells. *PLoS ONE* **9**, e88557 (2014). Medline doi:10.1371/journal.pone.0088557

22. A. C. Teng, N. A. Al-Montashiri, B. L. Cheng, P. Lou, P. Ozmizrak, H. H. Chen, A. F. Stewart, Identification of a phosphorylation-dependent nuclear localization motif in interferon regulatory factor 2 binding protein 2. *PLoS ONE* **6**, e24100 (2011). Medline doi:10.1371/journal.pone.0024100

23. A. C. Teng, D. Kuraitis, S. A. Deeke, A. Ahmadi, S. G. Dugan, B. L. Cheng, M. G. Crowson, P. G. Burgon, E. J. Suuronen, H. H. Chen, A. F. Stewart, IRF2BP2 is a skeletal and cardiac muscle-enriched ischemia-inducible activator of VEGFA expression. *FASEB J.* **24**, 4825–4834 (2010). Medline doi:10.1096/fj.10-167049

24. K. W. Jarosinski, P. T. Massa, Interferon regulatory factor-1 is required for interferon-gamma-induced MHC class I genes in astrocytes. *J. Neuroimmunol.* **122**, 74–84 (2002). Medline doi:10.1016/S0165-5728(01)00467-2

25. D. M. Pardoll, The blockade of immune checkpoints in cancer immunotherapy. *Nat. Rev. Cancer* **12**, 252–264 (2012). Medline doi:10.1038/nrc3239

26. W. Zou, L. Chen, Inhibitory B7-family molecules in the tumour microenvironment. *Nat. Rev. Immunol.* **8**, 467–477 (2008). Medline doi:10.1038/nri2326

27. J. Liu, A. Hamrouni, D. Wolowiec, V. Coiteux, K. Kuliczkowski, D. Hetuin, A. Saudemont, B. Quesnel, Plasma cells from multiple myeloma patients express B7-H1 (PD-L1) and increase expression after stimulation with IFN-gamma and TLR ligands via a MyD88-, TRAF6-, and MEK-dependent pathway. *Blood* **110**, 296–304 (2007). Medline doi:10.1182/blood-2006-10-051482

28. V. S. Salsman, K. K. Chow, D. R. Shaffer, H. Kadikoy, X. N. Li, C. Gerken, L. Perlaky, L. S. Metelitsa, X. Gao, M. Bhattacharjee, K. Hirschi, H. E. Heslop, S. Gottschalk, N. Ahmed, Crosstalk between medulloblastoma cells and endothelium triggers a strong chemotactic signal recruiting T lymphocytes to the tumor microenvironment. *PLOS ONE* **6**, e20267 (2011). Medline doi:10.1371/journal.pone.0020267

29. H. R. Seo, J. Kim, S. Bae, J. W. Soh, Y. S. Lee, Cdk5-mediated phosphorylation of c-Myc on Ser-62 is essential in transcriptional activation of cyclin B1 by cyclin G1. *J. Biol. Chem.* **283**, 15601–15610 (2008). Medline doi:10.1074/jbc.M800987200

30. S. C. Casey, L. Tong, Y. Li, R. Do, S. Walz, K. N. Fitzgerald, A. M. Gouw, V. Baylot, I. Gütgemann, M. Eilers, D. W. Felsher, MYC regulates the antitumor immune response through CD47 and PD-L1. *Science* **352**, 227–231 (2016). Medline doi:10.1126/science.aac9935

31. C. Twyman-Saint Victor, A. J. Rech, A. Maity, R. Rengan, K. E. Pauken, E. Stelekati, J. L. Benci, B. Xu, H. Dada, P. M. Odorizzi, R. S. Herati, K. D. Mansfield, D. Patsch, R. K. Amaravadi, L. M. Schuchter, H. Ishwaran, R. Mick, D. A. Pryma, X. Xu, M. D. Feldman, T. C. Gangadhar, S. M. Hahn, E. J. Wherry, R. H. Vonderheide, A. J. Minn, Radiation and dual checkpoint blockade activate non-redundant immune mechanisms in cancer. *Nature* **520**, 373–377 (2015). Medline doi:10.1038/nature14292